

Fractal dimension of spatially extended systems

A. Torcini^a, A. Politi^{a,b}, G.P. Puccioni^a and G. D'Alessandro^c

^a*Istituto Nazionale di Ottica, 50125 Florence, Italy*

^b*INFN-Sezione di Firenze, Florence, Italy*

^c*Physics Department, University of Strathclyde, Glasgow, UK*

Received 29 October 1990

Revised manuscript received 21 March 1991

Accepted 20 April 1991

Communicated by A.C. Newell

Properties of the invariant measure are numerically investigated in 1D chains of diffusively coupled maps. The coarse-grained fractal dimension is carefully computed in various embedding spaces, observing an extremely slow convergence towards the asymptotic value. This is in contrast with previous simulations, where the analysis of an insufficient number of points led the authors to underestimate the increase of fractal dimension with increasing the dimension of the embedding space. Orthogonal decomposition is also performed confirming that the slow convergence is intrinsically related to local nonlinear properties of the invariant measure. Finally, the Kaplan–Yorke conjecture is tested for short chains, showing that, despite the noninvertibility of the dynamical system, a good agreement is found between Lyapunov dimension and information dimension.

1. Introduction

Low-dimensional chaos is a fairly well understood topic [1]. In particular, it is well known that the invariant measure associated with a strange attractor can be exhaustively characterized by means of a multifractal formalism [2]. However, many results refer to the simplest possible case: two-dimensional maps with an expanding and a contracting direction. The understanding is already less satisfactory when passing to a three-dimensional phase space with a 2D stable manifold. In such a case it is not even clear whether the attractor is fractal along only one direction, as often conjectured [3]. If this were the case, multifractality would play a negligible role in high dimensional attractors. On the other side we can ask ourselves if, in the limit of infinite-dimensional systems (thermodynamic limit), the invariant distribution can be described in terms of new scaling relations, because of the spatial homogeneity of fully developed spatio-temporal chaos.

The basic ideas, so far developed, rely upon the concept of limit spectrum of Lyapunov exponents and density of dimensions: two straightforward generalizations of well known indicators, introduced to describe low-dimensional chaos. Let us define them for a system with discrete space (i) and time (t) variables. There is numerical and preliminary analytical evidence of the existence of a limit spectrum,

$$\Lambda(\sigma) = \lim_{I \rightarrow \infty} \lambda(\sigma I, I), \quad (1.1)$$

where $\lambda(j = \sigma I, I)$ is the j th largest Lyapunov characteristic exponent for a lattice with I sites [4]. The existence of such a limit immediately leads to conjecture that the dimension $D(I)$ is an extensive quantity, so that the density of dimension $\rho \equiv D(I)/I$ is independent of I . The meaning of this last relation is that, loosely speaking, the dynamics of a very long chain can be interpreted as that of many juxtaposed independent

pieces of large enough length L . By pushing farther on this argument, Grassberger [5] was led to conjecture that a finite portion of an in principle infinite chain exhibits a dimension equal to ρL ($< L$) for L large enough. More precisely, by calling x_t^i the state variable, and building an L -dimensional vector $V_t(i) \equiv (x_t^i, x_{t+1}^i, \dots, x_{t+L-1}^i)$ for each site i , it is expected that the V_t 's fill the space with an invariant measure of dimension equal to $\rho_s L$ (the subscript s indicates that the embedding space is constructed with reference to spatial dependence). As a consequence it should be possible to distinguish a truly random noise (where $D(L) = L$) from a deterministic signal arising from an extended system.

The same conjecture has been extended to the time domain [5, 6] by constructing vectors $V_t(i) \equiv (x_t^i, x_{t+1}^i, \dots, x_{t+L-1}^i)$ (i.e. by using a standard temporal embedding procedure). In this latter case let us remark the difference with respect to low-dimensional chaos where $D(L)$ converges, for increasing L , to some finite value which is interpreted as the dimension of an underlying attractor. In the present case, instead, no saturation is expected, but the growth rate of $D(L)$ is again conjectured to be strictly smaller than one for extended systems. In ref. [6] an attempt has been made to express the temporal dimension density ρ_t in terms of dynamical invariant indicators.

More recently, preliminary simulations have been presented [7] showing that some of the relations conjectured in refs. [5, 6] are not entirely correct, as they are essentially based on finite-size estimations of fractal dimensions. It is our aim to show here that careful estimates of fractal dimension in chains of coupled maps indicate that both spatial and temporal embedding lead to a dimension coinciding with that of the embedding space (as for random signals) provided that a sufficiently large number of points has been used. We can see this by following a general argument. Assuming that the dynamics of the map lattice is mixing (this is reasonably true

for fully developed spatio-temporal chaos) it follows that the distribution of $V_t(i)$ values taken at the same time t , in different sites i , is the same as the distribution of values taken in the same site at different times. The distance $d_L(i, t', t'')$, between two sequences $V_{t'}(i), V_{t''}(i)$ in an embedding space of dimension L , is nothing but the distance between the projections in a suitable L -dimensional subspace of the original points (i.e. with all variables taken into account). In other words, the dimension $D(L)$ of a sub-chain of length L is the dimension of the projection of a suitable $\rho_s L$ -dimensional subset onto a (generic) subspace of dimension L . As $\rho_s L > L$, we must in general expect $D(L) = L$, except for very exceptional cases.

Nevertheless, behind this seemingly obvious conclusion, we have numerically observed the less trivial fact that the resolution one needs to reach in order to observe the saturated asymptotic value diverges in the thermodynamic limit $L \rightarrow \infty$. Accordingly, in some sense, we can recover the conclusions reported in refs. [5, 6], by claiming that the coarse-grained (i.e. finite resolution) dimension grows linearly with L , with a slope strictly smaller than 1. However, the problem of characterizing the invariant measure of a map lattice is now more cumbersome as the dependence on two relevant scaling parameters must be simultaneously taken into account. In section 3 we discuss this problem and introduce some very preliminary conjecture.

In section 2 we present the numerical simulations by discussing various tricks to decrease the finite-size effects and to speed up the comparison of relative distances. It is important to mention that we have also performed a change of variables, by recurring to the orthogonal decomposition, to check the stability of our results (section 4). In section 5 we compare our analysis with previous papers, presenting an alternative interpretation of the numerical results and substantiating the criticisms outlined in this introduction. As all of our numerical analyses refer to coupled logistic maps, that is to a noninvertible dynamics,

we have also performed some computations in short length chains to test the Kaplan–Yorke conjecture, which is not necessarily expected to hold. Our results indicate that if there is any difference between the Lyapunov dimension and information dimension, it stays finite for increasing length l (section 6).

2. Numerical simulations

We have iterated the standard model of a 1D lattice of coupled logistic maps [8],

$$x_{t+1}^i = a - (y_t^i)^2, \quad (2.1)$$

where

$$y_t^i = \frac{1}{2}\varepsilon x_t^{i-1} + (1 - \varepsilon)x_t^i + \frac{1}{2}\varepsilon x_t^{i+1} \quad (2.2)$$

schematizes a diffusive coupling. The parameter ε controlling the strength of the coupling, is bound between 0 (uncoupled case) and 1 (two independent space–time lattices). Periodic boundary conditions (i.e. $x_t^0 = x_t^l$, $x_t^l = x_t^{l+1}$) have always been used throughout our paper, unless explicitly stated otherwise.

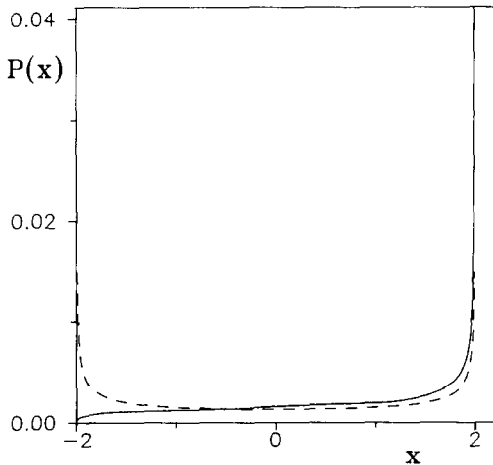


Fig. 1. Invariant probability distribution $P(x)$ for a chain of coupled logistic maps with $\varepsilon = \frac{2}{3}$ and $a = 2$ (full curve) compared with the probability distribution of the single map (dashed curve).

The fractal dimension has been computed by means of the nearest-neighbour method [9] which is based on the comparison of a randomly chosen reference point with an increasing number n of data points (randomly chosen too). The logarithm of the distance of the k th nearest neighbour for different n -values is then averaged over m different reference points to decrease the statistical error as much as possible. Therefore, the number n of data points controls the length scale (larger n values yield smaller distances), while the number m of reference points controls the statistical error on the distance $\delta(k, n)$. From the scaling behaviour of the distance with n ($\delta(k, n) \simeq (k/n)^{-1/D}$ [9], where D is the information dimension), it follows that

$$D_{\text{cg}} \equiv -(\text{d} \ln n / \text{d} \ln \delta) \quad (2.3)$$

can be interpreted as a coarse-grained dimension.

All of our numerical simulations refer to the case $\varepsilon = \frac{2}{3}$ and $a = 2$, where the dynamics of the single map is at the Ulam point with invariant measure $P(x) = 1/2\pi\sqrt{4-x^2}$ characterized by two square root singularities at the extrema of the invariant interval $[-2, 2]$. For comparison we have plotted in fig. 1 the invariant single site distribution for the chain of maps, where only one singularity is present on the right, deriving from the existence of a quadratic maximum in the map. Indeed, assuming a flat distribution around the preimage of the maximum of eq. (2.1), a singularity with exponent $\beta_1 = -\frac{1}{2}$ is necessarily generated around $x = 2$. A careful numerical analysis around the minimum value $x = -2$ shows that $P(x)$ goes instead to zero with a scaling exponent $\beta_2 \simeq \frac{1}{3}$. This remarkable difference with respect to the single-map case (where $\beta_2 = -\frac{1}{2}$ is found) can be qualitatively explained. In fact, the minimum value $x = -2$ is reached at time $t + 1$ if and only if a sequence of three maxima is observed at time t . Assuming x_t^i to be independent of x_t^{i+1} , and using the local linearity of the map around $x = 2$ with an expansion coefficient 4, it

follows that

$$(\delta x)^{1+\beta'_2} = [P(x=2)^{\frac{1}{4}}\delta x]^3 \equiv (\frac{1}{4}\delta x)^{3(1+\beta_1)},$$

from which an exponent $\beta'_2 = \frac{1}{2}$ is found, explaining the convergence to zero of $P(x)$. In fact, one can easily see that the contribution coming from the mass remaining around the minimum value $x = -2$ is negligible. The difference between β'_2 and the actual value $\beta_2 \approx \frac{1}{3}$ is presumably to be attributed to correlations between nearby sites.

The relevant point emerging from the analysis of the invariant measure is the occurrence of a spike around $x = 2$. Such a singularity does not affect any generalized dimension D_q with q strictly smaller than 2, as shown in ref. [10]. In particular it does not affect the information dimension computed with the nearest-neighbour algorithm. However, this is rigorously true only in the limit of infinite resolution. Since numerical simulations allow one to investigate only a limited range of distances, and such a range becomes increasingly small for increasing dimension, it is crucial to smooth out as much as possible the localized peaks in the distribution heavily affecting D_{cg} . Therefore, we have performed a change of coordinates (with a singularity at the upper edge) from x to z , such that the z -probability density $Q(z)$ was constant. Such a change of variable does not affect the asymptotic value of the information dimension.

A second important reduction of finite-size effects can be achieved by decreasing the edge effects. In the literature, some papers have appeared which deal with this problem [11]. They mainly refer to “trivial” edges like those of a hypercube S in case of a uniform invariant measure. In such a case, the average density in a sphere of radius δ , centered around a point distant r from the S -edge, turns out to be obviously underestimated as long as $\delta > r$. This, in turn, leads to an underestimation of the dimension. The offset becomes more and more relevant for increasing dimensions, as already discussed in ref.

[12]. However, it is possible to reduce it by simply changing the topology of the L -dimensional phase space. By identifying opposite edges, the hypercube is transformed into a torus T^L : a mapping which, while leaving the dimension unchanged, removes all the empty regions responsible of the underestimation effect. Such a trick can be easily implemented on a computer, especially when working with integer numbers. By using for instance 27000 points in a six-dimensional space (averaging over 3000 reference points, and looking at the 20th nearest neighbour), we have obtained $D = 6$ with an error around 0.1, to be compared with the underestimation $D \approx 5.47$ obtained from the original data points.

Obviously, this idea proves to be very effective in the case of independent and equally distributed variables, since all empty regions are removed. It is expected to be less powerful in the case of coupled maps, where correlations both induce nonuniformities in the probability distribution and open gaps, which can, in principle, cause either under- or over-estimations of the dimension. The relevance of edge-effects is confirmed by the analysis of the two-dimensional distribution $P(x, y)$ for two adjacent sites x, y . Its support covers only a subset of the allowed square, as seen from fig. 2, where exponentially separated contour lines of $P(x, y)$ are plotted. In order to further increase the accuracy of our simulations, we have performed another change of variables, by expanding such a support to the whole square. Obviously, we still expect edge effects to arise because of third and higher order correlations, yielding empty regions in higher dimensional spaces.

The last trick regards the implementation of the numerical algorithm. We have extended to the nearest-neighbour approach, the method proposed by Theiler [13] for the Grassberger–Procaccia algorithm [14]. The main idea is to introduce a coarse grained fixed size partition in the space of minimum embedding dimension L_{min} we work with. It allows us to organize the points into hypercubes (or boxes). This can be done very

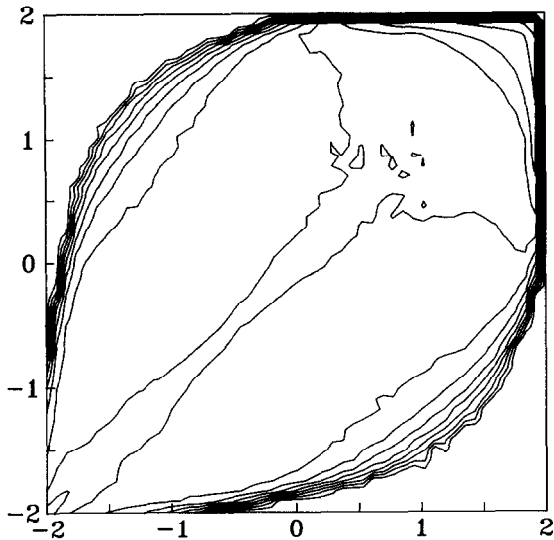


Fig. 2. Exponentially separated contour lines of the probability distribution $P(x, y)$ on two adjacent sites (same parameter values as in fig. 1).

efficiently by creating a vector of pointers, where each element is the index of another point falling in the same box (if there is one). Now, if one uses the maximum norm and is interested in distances smaller than the size of the grid, it is sufficient to compare each point with those ones falling in the same, or in a neighbouring box (for any embedding dimension $L > L_{\min}$). In this way the majority of large distances are not computed a priori, thus saving a lot of CPU-time. However, because of the consequent speed in the execution of this code, one encounters another bottleneck due to storage limitations. It is no longer possible to store simultaneously all the points in the central memory, so that one is forced to proceed in terms of blocks, each one separately randomized and fitted in the grid.

The above discussed method is more effective for grids of small size, as many pairs of points are automatically discarded. However, we are faced with the difficulty of generating a large number of points in order to have sufficient statistics. Another way to cut a priori a larger number of distances requires to choose L_{\min} as large as possible, at the expense of decreasing the number

of embedding dimensions simultaneously processed. With our computer (HP-835) a reasonable compromise has been achieved by fixing $L_{\min} = 5$, as the standard approach allowed us a complete analysis for smaller dimensions. Finally, we have split each linear dimension into eight parts, thus dividing the points into 2^{15} different boxes.

The results for the behaviour of the 10th neighbour are summarized in fig. 3 for different embedding dimensions L (namely, 3, 4, 5, 6, 7, and 9) averaged over 45 000 reference points. As the improved algorithm allows us to determine D_{cg} only at relatively small distances, we have also reported the outcome of the standard algorithm (which allowed us to arrive at 2.7×10^6 points, compared with 10^8 points reached with Theiler's algorithm). As a check, we have also monitored, during the simulation, the 4th and 30th neighbour, obtaining very similar results. Notice that, notwithstanding the choice of a different norm (sum of absolute values and maximum for the standard and improved algorithm, respectively) the curves essentially agree in the overlapping region. The only exception is represented by the case $L = 9$, as the outcome of the new program is affected by the following defect. As long as the distance of the k th (10th in the present case) neighbour is greater than the grid size, it is overestimated, as many points have been discarded during the computation. As a consequence, if n is not sufficiently large, we have to expect an underestimation of D_{cg} , as observed in the case $L = 9$ for small n 's.

The estimate of the coarse-grained dimension is affected by two different kinds of error due to the average over a finite number m of reference points, and to the usage of a finite number of nearest neighbours. The amplitude of the first kind of error can be inferred from the size of the fluctuations exhibited by D_{cg} . For an estimate of the second kind of error see fig. 6 below.

At embedding dimensions $L = 3, 4$ and 5 , a saturation of D_{cg} to a value coinciding with the space dimension is clearly observed. For $L = 6$, D_{cg} arrives at most at 5.7 , but no evidence of

convergence to an asymptotic value is revealed, so that this value still appears as an underestimation. It is instructive to notice that the various tricks adopted to obtain the result plotted in fig. 3 for $L = 6$ lead to an increase of D_{cg} of about 1.5 with respect to the straightforward application of the nearest-neighbour method (for the same number of points). This indicates the relevance of finite size corrections. Therefore, we are quite confident that the lack of convergence observed for $L = 6$ is mainly due to higher order edge effects that we could not eliminate. The cases $L = 7$ and 9 confirm the increasing difficulty to reach the asymptotic value for increasing L . The difference between the embedding dimension and the largest observed D_{cg} is still around 1.8 for $L = 9$, but again no evidence of convergence is exhibited. Therefore, our conclusions point in the direction of suggesting that the equality $D(L) = L$ holds, indicating that the results shown in refs. [5, 6] follow from the choice of a finite and constant number of data points.

For completeness, we have investigated the temporal embedding case as well, proceeding exactly in the same way as for the spatial case. Namely, we have changed the variable x to make the single-site invariant measure uniform. Then we have extended the two-dimensional domain to the whole square and changed the space topology. In this case, it is possible to derive analytical approximations to the support of the 2D distribution (see ref. [7]). The results are plotted in fig. 4. They are very similar to those for spatial embedding displayed in fig. 3.

3. Interpretation

An important question about the numerical results discussed in the previous section concerns the justification of the observed slow convergence. In particular we would like to discover whether the underestimation is essentially due to the trivial fact that the number of points used to

estimate the dimension must be increased when looking at sets of increasing dimension, or to some intrinsic property of the invariant measure. In ref. [6], the authors tried to link the fractal structure with dynamical invariants like Lyapunov exponents, generalizing the ideas behind the Kaplan–Yorke conjecture in finite dimensional attractors. In section 5 we present some objections to their arguments. For the moment we start with an empirical approach. From the theory of multifractal sets, we can reasonably assume that the average mass $p = k/n$ in a box of radius ε (we recall that k being the neighbour-order, can also be interpreted as the number of points in the box) behaves as

$$p \simeq a\varepsilon^D(1 + b\varepsilon^{cD}), \quad (3.1)$$

where D is the information dimension and $D(1 + c)$ describes the leading scaling behaviour of corrections. Such exponents should correspond to the two largest eigenvalues of a suitable operator. Although in the present case we have not enough elements to verify this hypothesis, it is at least reasonable to conjecture that eq. (3.1) holds for the invariant measures we are looking at. From the definition of coarse-grained dimension D_{cg} given in (2.2) and from the relation between p and n we can write

$$D_{\text{cg}} \equiv \frac{d \log p}{d \log \varepsilon} \quad (3.2)$$

(ε plays the role of δ in eq. (2.2)). From eq.(3.1) we obtain

$$D_{\text{cg}} = D[1 + (1 + c)b\varepsilon^{cD}], \quad (3.3)$$

where we have retained the leading terms in the series expansion. As our simulations refer to the nearest-neighbour method, where the scaling parameter is the number of points $n = \varepsilon^{-D}$, eq.

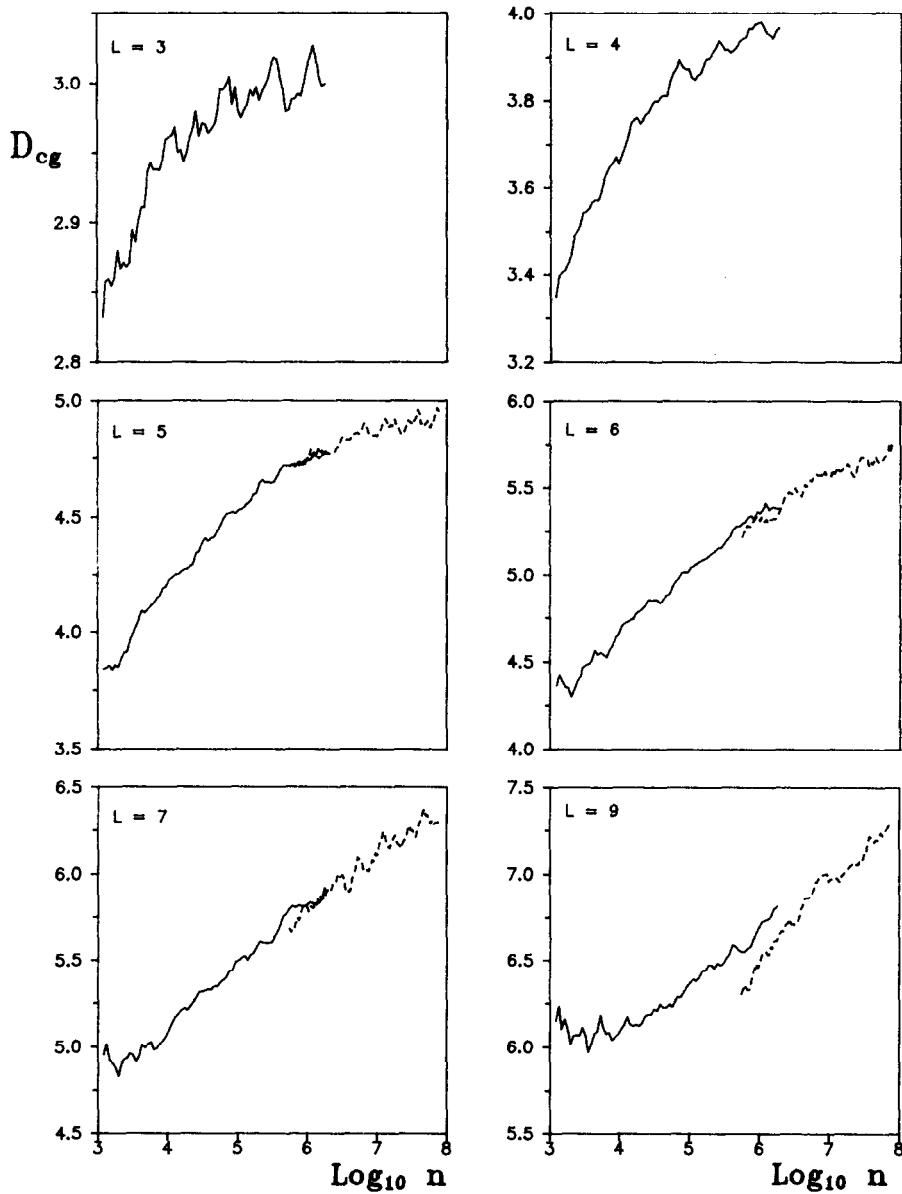


Fig. 3. Coarse grained dimension from spatial embedding technique as a function of the decimal logarithm of the number of points for the 10th nearest neighbour, averaged over 45000 reference points. Dashed curves refer to the improved method, full ones to the standard algorithm.

(3.3) can be rephrased as

$$D_{cg}(L, n) \approx L[1 + (1 + c)bn^{-c}], \quad (3.4)$$

where we have substituted D with L , as the asymptotic dimension coincides with that of the

embedding space. Practically, we expect higher order correction terms to be present in eq. (3.1), so that eq. (3.4) is only approximately valid. In particular, whenever the observed D_{cg} is far from asymptotic, only a qualitative agreement can be expected. By fitting the numerical results (par-

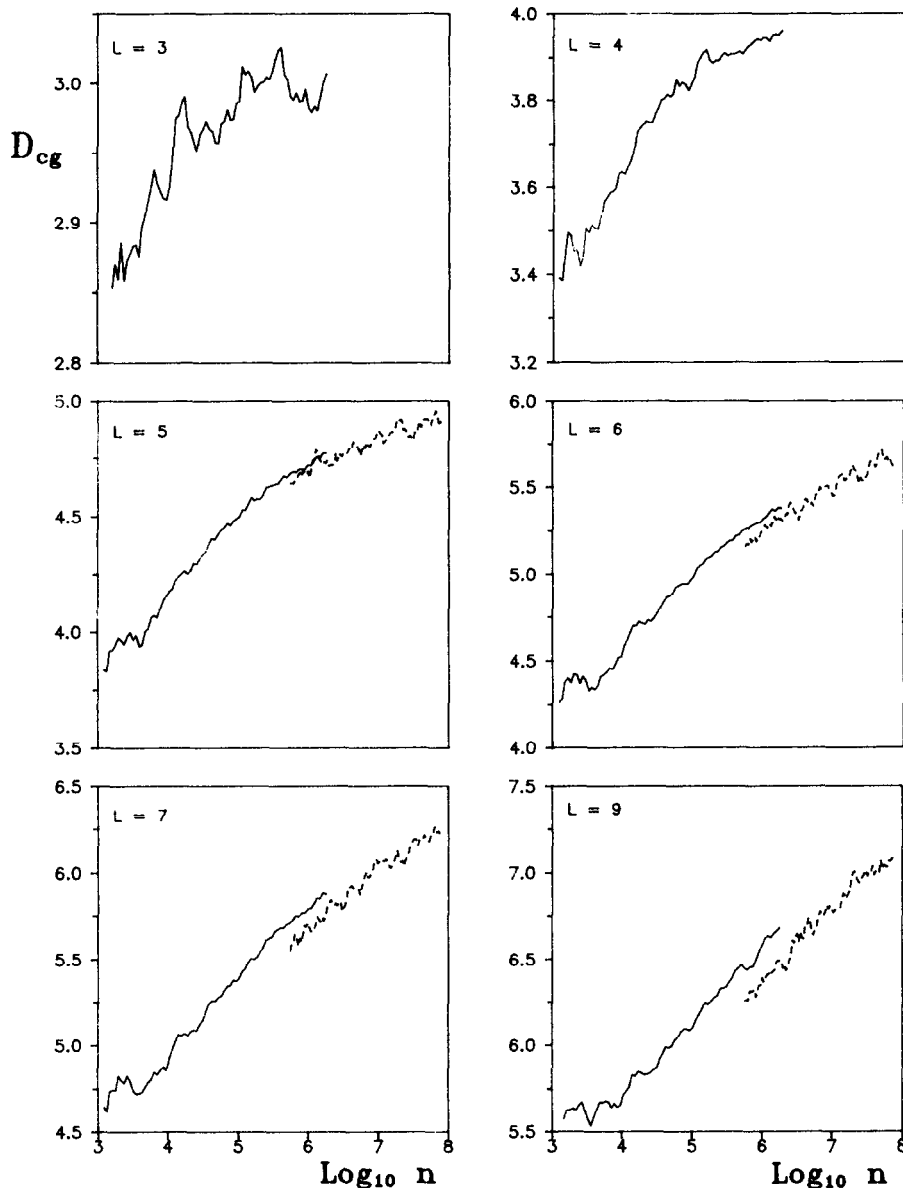


Fig. 4. Same as in fig. 3, referred to temporal embedding.

tially presented in figs. 3, 4) with expression (3.4), where b and c are the only free parameters, we can extrapolate the minimum number of points n^* needed to observe $D_{cg} = (1-f)L$,

$$n^* = \left(-\frac{b(c+1)}{f} \right)^{1/c}. \quad (3.5)$$

In fig. 5 we report the result of the fit with eq.

(3.4) for $L = 7$, spatial embedding, and the 10th neighbour, compared with numerical data. The good agreement indicates that the functional choice made in eq. (3.4) is very reasonable. Moreover, despite the large uncertainty associated with the extrapolation of n^* for $L = 8, 9$, the results for the parameters b, c are very stable. Practically, there are no differences with respect to the estimates obtained in ref. [7] with fewer data.

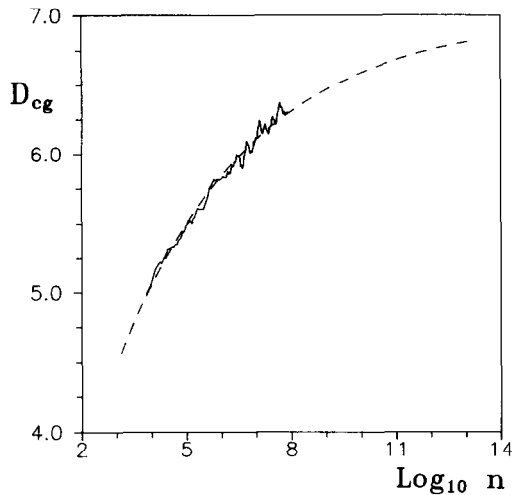


Fig. 5. D_{cg} versus $\log_{10}n$ for the 10th neighbour, $L = 7$ from spatial embedding. Numerical results (continuous line) are compared with the fit (dashed curve).

In order to have a more objective indicator (n^* depends on the order of the neighbour considered in the analysis), we passed from the number of points n^* to the critical distance ε^* , by integrating eq. (3.4),

$$\varepsilon = Kn^{-1/L} [1 + (1+c)bn^{-c}]^{1/cL}, \quad (3.6)$$

where K is the integration constant to be determined with a further fit, $n^{-1/L}$ yields the expected asymptotic behaviour, and the last multiplicative factor controls the finite size corrections. We can determine ε^* , by substituting eq. (3.5) in eq. (3.6)

$$\varepsilon^* = K \left[-\frac{b(1+c)}{f} \left(1 - \frac{(1+c)^2 b^2}{f} \right) \right]^{1/cL}. \quad (3.7)$$

ε^* represents the maximum average distance one can reach still observing the asymptotic scaling behaviour with accuracy f . In fig. 6 we have plotted $\log \varepsilon^*$ versus L , for all neighbour orders computed in our simulations (i.e. 4, 10 and 30) and with $f = 0.03$. The results in fig. 6 indicate a

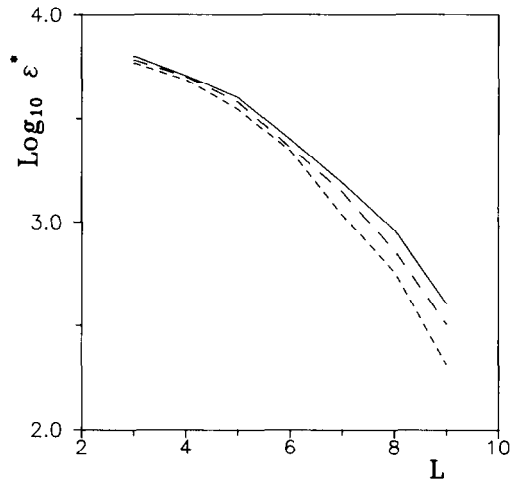


Fig. 6. Logarithm of the critical distance ε^* required to observe the asymptotic value of the fractal dimension versus the dimension of the embedding space L . Full, dashed and dotted curves refer to the 4th, 10th and 30th neighbour, respectively.

fast decrease of $\log \varepsilon^*$ for increasing L . However, it is almost impossible to understand whether the asymptotic behavior is linear or faster. In principle, one should go to higher embedding dimensions, but the extrapolations would become less and less reliable. The difference among the three curves in fig. 6 is a qualitative measure of the error (ε^* should in fact be independent of k) which is rather large already for $L = 9$. The only way to keep the error under control, is to increase the number of points. However, this alternative soon becomes unfeasible: in order to reach $D_{cg} = 8.7$ for $L = 9$, one needs 10^{22} points. As a consequence, from our simulations, we cannot exclude the existence of quadratic effects.

A possible explanation of our results can still be based on trivial edge effects which have not been completely removed. In fact, it is important to study their scaling dependence on L . We present a calculation in the case of a hypersphere. The results should not vary significantly for different but not too strange geometries. This seems to be the case as the estimated dimension D coincides with the dimension of the embedding space. Let

R, r be the radii of the sphere, respectively of the generic ball used to estimate the local probability density, which we assume to be uniform, for simplicity. The fraction p of balls (randomly chosen), whose mass is affected by the presence of empty regions, is obviously given by the fractional volume of the sphere contained between the radii $R - r$ and R . For $r \ll R$ we obtain

$$p = L(r/R). \quad (3.8)$$

The fraction p has to be kept constant for increasing L values, if we want to keep the underestimation error under control. As a result, the range of distances one has to reach to fulfil this condition goes to zero as p/L . Hence, contrary to what is usually believed, we see that already in this naive case, with uniform distribution, the number of points must grow faster than exponentially in L , namely

$$N = (L/p)^L. \quad (3.9)$$

Let us recall the standard argument used to determine the minimum number of points required to estimate a given dimension value. Assuming that the distance among points along any direction has to be smaller than a given fraction g of the actual size of the attractor, we must at least generate $N = g^{-L}$ points to fulfil such a condition along all directions. Ruelle and Eckmann have been able to prove that such a limit can be reduced to $N = g^{-L/2}$ in the case of Grassberger–Procaccia algorithm, noticing the peculiarity of that method [15]. Indeed, the counting procedure is formally equivalent to computing all distances from a single fictitious reference point around which the distributions seen from any reference point, are rigidly shifted and overlapped. As a result, we have an “equivalent” number of points around the fictitious reference one which is half of the square of the number of effective available points, thus accounting for the square root factor found in ref. [15]. However, eq. (3.9) indicates that a more dangerous problem

can arise from the border of the support of the probability density.

Coming back to our simulations, the factor-10 increase of the minimal resolution, when passing from $L = 4$, to $L = 9$, cannot be entirely explained by the edge effect which accounts only for a factor $\frac{9}{4}$ (see eq. (3.8)). A plausible explanation is that the thickness of the invariant set (projected onto an L -dimensional space) becomes smaller and smaller along some directions for increasing L . We investigate this point in the next section, by introducing suitable global coordinates by means of the orthogonal decomposition.

We end this section by studying the dependence of the scaling parameter c on L . In fig. 7, $1/c$ is plotted versus L indicating a parabolic shape. By substituting this empirical result in eq. (3.1), we notice that the relative amplitude of the finite-size corrections scales as $\varepsilon^{s^2/L}$ (recalling that $D = L$ and being s the quadratic coefficient of the curve in fig. 7). By redefining $\varepsilon^*(g)$ as the distance to reach in order to have a finite size correction g , we have

$$\varepsilon^*(g) = \exp\left[\frac{L}{s^2} \log\left(\frac{g}{b}\right)\right]. \quad (3.10)$$

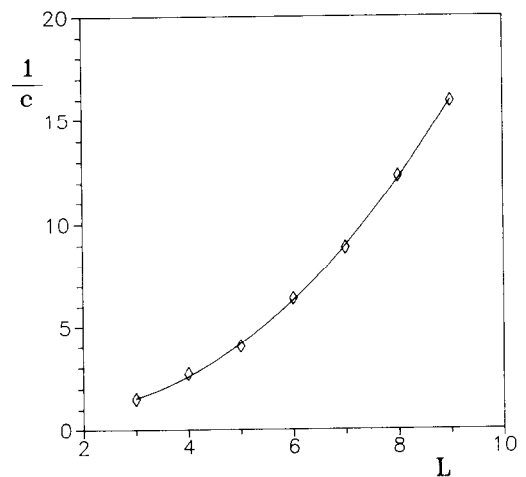


Fig. 7. Inverse of the scaling parameter c (see eq. (3.1)) versus L (diamonds), fitted with a parabola (continuous curve).

In other words, we find again that the critical resolution ε^* scales exponentially with L , thus reinforcing this conjecture. Notice, however, that the results presented in fig. 7 are much more reliable as they are not based on somehow arbitrary extrapolations as for the results in fig. 6. Furthermore, from eq. (3.10), we can see that the decay rate $-\log(g/b)/s^2$ depends on the accuracy g . This is equivalent to saying that the slope of the curves in fig. 6 should increase for decreasing f (analogous to the parameter g). Measurements made for several f values are qualitatively in agreement with these findings.

4. Orthogonal decomposition

So far we have discussed the implementation of various tricks to improve the convergence of D_{cg} to the asymptotic value, by always referring to the same set of variables. Obviously, the fractal dimension should be independent of the choice of coordinates in the limit of infinite resolution. However, when working with boxes of finite size, the deviations from the asymptotic result might heavily depend on the variables chosen to parametrize the phase space. Therefore, the determination of an optimal reference frame can play a relevant role in performing accurate dimension estimates. In general, we always expect a suitable nonlinear change of variables to exist such that the finite-size corrections are negligible. Unfortunately, in general, the construction of such a set of coordinates can be accomplished only a posteriori, after having determined the local scaling behaviour around each point. In this section, we follow a simpler scheme considering only linear changes of coordinates, in the spirit of ref. [16, 17]. In other words, we discuss the possibility to unravel the structure of the invariant measure in a given embedding space, by expressing each state in terms of suitable global modes (like e.g. Fourier modes). To this aim we introduce the orthogonal decomposition, whose meaning is as follows. Starting from a given distri-

bution in an L -dimensional space (whose center of mass is assumed to be in the origin, for simplicity), we first determine the direction along which the average projection of a generic state is maximal. By further projecting the distribution onto the $(L-1)$ -dimensional subspace, which is orthogonal to the direction just found, we can repeat the procedure determining a second vector, and so on until a 1D space is reached. As an example, let us consider a uniform distribution in a 3D space restricted to an oblique thin sheet. It is obvious that for distances larger than the thickness of the set, the dimension is underestimated. There is no way to increase the critical distance ε^* by renormalizing the coordinates. The above outlined method allows us to define a new set of variables (x, y, z) , with z being the direction of small thickness. Upon further rescaling all of the three new variables (i.e. transforming the parallelepiped into a cube), it is immediately seen that one can observe $D_{cg} = 3$ already at large distances. Such a method proves to be very effective in this simple example because of the ‘‘linearity’’ of the subspace. More in general, we can expect it to work in all cases where nonlinear deviations are weak. The implementation of the algorithm is quite straightforward, as the new base can be determined by diagonalizing the correlation operator

$$K_{i,j} \equiv \langle x_n^i x_n^j \rangle, \quad (4.1)$$

where $\langle \cdot \rangle$ indicates time average [16]. More precisely, we can write

$$x_n^i = \sum_{k=1}^L A_{n,k} \psi_k^i \quad (4.2)$$

where ψ_k^i is the i th component of the k th eigenvector of $K_{i,j}$. These vectors, altogether, represent an orthonormal base. One can also prove that

$$\langle A_{n,k} A_{n,m} \rangle = \lambda_k \delta_{k,m}, \quad (4.3)$$

where $\delta_{k,m}$ is the Kronecker δ -function and λ_k is the k th eigenvalue of $K_{i,j}$. Furthermore λ_k represents the energy of the k th mode ψ_k^i , that is the averaged square size of the subset along ψ_k^i . Such a method has been applied very recently to various problems of turbulence (Rayleigh–Bénard convection, Navier–Stokes equations, Kuramoto–Sivashinsky equation) and even to experimental data [18]. In ref. [18], the authors conjecture that the method is so powerful that it might represent a feasible alternative to the application of standard algorithms to compute the fractal dimension. In fact, they found a good agreement between the correlation exponent (computed by means of Grassberger–Procaccia algorithm) and the number of modes containing a given fraction (arbitrarily chosen equal to 93%) of the whole energy. If this were true, it would imply that the invariant distribution covers an essentially linear subspace. We do not aim to discuss here such a thesis, rather we are interested in applying this method to the embedding procedure. Therefore we again consider subchains of length L (for sake of brevity we investigated $L = 8$ only). Let us first recall that in the case of periodic boundary conditions and uniform spatio-temporal chaos, orthogonal decomposition leads to the well known Fourier modes. This is precisely our case, with the only difference that periodicity is lost when considering subchains. Nevertheless, as the boundary conditions are expected to become less and less important for long chains, the global modes turn out to be very close to Fourier modes.

In a few words, starting from spatial subchains of length $L = 8$, we computed the correlation operator and its eigenmodes. After subtracting the average state, we have projected the vectors onto such a base, separately making uniform the distribution of all the eight amplitudes. The results of the computation of D_{cg} in this new space are reported in fig. 8. It is clearly seen that a big increase with respect to the standard approach is observed at small n -values, whereas at larger n 's the new curve is even lower than the previous one. This means that at “large” distances the

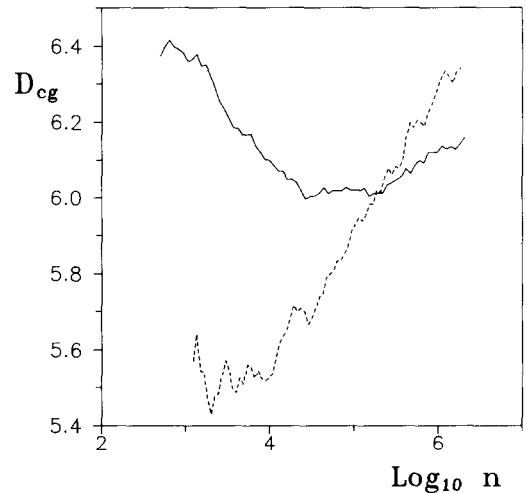


Fig. 8. Fractal dimension D_{cg} for spatial embedding ($L = 8$) from the distance of the 10th neighbours: in real space (dashed line), and after orthogonal decomposition (continuous line).

invariant measure roughly fills a linear subspace (notice however that D_{cg} still remains well below the space dimension). The inversion occurring at larger n 's is presumably due to the fact that the new results have been obtained without removing 2D edge effects (the size of such effects is in fact comparable with the distance between the two curves). As a consequence we are led to conclude that the slow convergence of D_{cg} is intrinsic and due to genuine nonlinear effects.

The method of orthogonal decomposition can also be applied to the temporal sequence. In this case, it corresponds to the well known singular value decomposition introduced in ref. [19]. This procedure was introduced to filter out the noise present in experimental data. It is implicitly based on the assumption that the invariant measure fills a linear subspace. Any small deviation from such a condition is considered as an experimental artifact and, therefore, corrected. Except for peculiar cases, such a method is not very effective, as already pointed out in refs. [12, 20].

Here, in some sense, we apply this method with the opposite goal: expanding the distribution along those directions which correspond to small thicknesses, in order to increase the observational

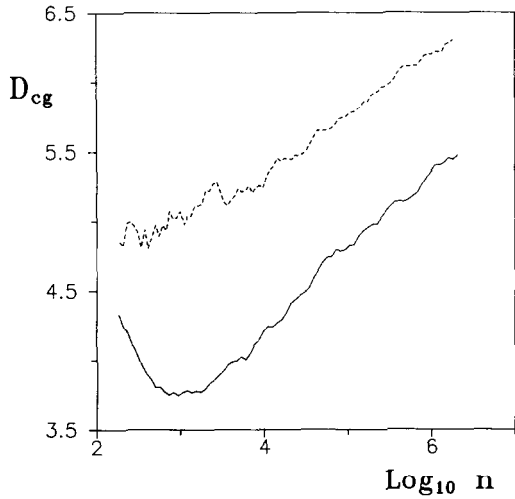


Fig. 9. Same as in fig. 8, for temporal embedding.

resolution. The results of the simulations are reported in fig. 9. The D_{cg} curve lies everywhere below the curve obtained in section 2 by using the original set of coordinates. This means that non-linear effects are even stronger than in the spatial case and indicate that a local analysis is requested to better understand the slow convergence of the fractal dimension.

5. Comparison with previous results

In the previous sections we have been able to conclude that the difficulty of estimating the fractal dimension in spatially extended systems is due to the particular structure of the invariant measure. Its projection onto lower dimensional spaces is presumably locally very narrow along some directions. We want now to interpret our findings in the framework of ref. [21]. To this aim, we rephrase the arguments of Mayer-Kress and Kurz. Let x_t denote the temporal evolution of a chain of I coupled maps observed in a reference point (we are assuming spatially homogeneous chaos). We can formally write

$$x_t \equiv x_t^{(1)}(T) + \sum_{i=1}^{I-1} [x_t^{(i+1)}(T) - x_t^{(i)}(T)], \quad (5.1)$$

where $x_t^{(i)}(T)$ indicates the best approximate to the evolution of x_t (over a time $0 < t < T$) chosen among the trajectories of length T of a chain of i maps. Therefore, we can interpret $\delta_t^{(i)}(T) \equiv x_t^{(i)}(T) - x_t^{(i-1)}(T)$ as the perturbation to the dynamical behavior following from the addition of one site to the chain. In dissipative systems, where the volume is contracted to 0, we can assume that $\delta_t^{(i)}(T)$ goes to zero for $i \rightarrow \infty$. It is not at all a trivial task to study such a limit, especially for T tending to infinity (for instance, it is not clear whether $\delta_t^{(i)}(T)$ goes uniformly to zero for all t 's). In ref. [21], relying upon a conjecture raised by Pomeau [22], it has been assumed that, independently of T ,

$$\|\delta_t^{(i)}\| \approx \exp(-i/l_c) \quad (5.2)$$

for i large enough, where l_c is a characteristic length estimating the decay rate of the influence of points at increasing distance from the reference site. By assuming that distances smaller than ε cannot be resolved, the sum in eq. (5.1) can be truncated at the $m(\varepsilon)$ th term, where m and ε are related by the equation

$$\varepsilon = \exp[-m(\varepsilon)/l_c]. \quad (5.3)$$

Accordingly, the evolution of the chain can be approximated, within such an accuracy, by that one of an $m(\varepsilon)$ -dimensional chain. The fractal dimension $D(\varepsilon)$ of the associated attractor is nothing but

$$D(\varepsilon) = \rho m(\varepsilon), \quad (5.4)$$

where ρ is the dimension density. Therefore, the coarse-grained dimension $D_{cg}(\varepsilon, L)$, estimated in an L -dimensional embedding space, is given by

$$D_{cg}(\varepsilon, L) = \rho m(\varepsilon), \quad D(\varepsilon) \leq L, \\ = L, \quad D(\varepsilon) > L.$$

As a consequence, the resolution ε^* such that $L = \rho m(\varepsilon^*)$ corresponds to the maximal distance

still yielding $D_{\text{cg}} = L$. Upon substituting in eq. (5.3), we have

$$\varepsilon^* = \exp(-L/\rho l_c) \quad (5.5)$$

exhibiting the same exponential law numerically found in section 3. The exponent α is related to l_c , as

$$\alpha = 1/\rho l_c. \quad (5.6)$$

Let us now investigate the origin of the decay of $\delta_i^{(i)}$ for increasing i . The addition of one or more sites to a chain of length L can be seen as the coupling of the original L -dimensional dynamical system with a thermal bath. The external noise, loosely speaking, dresses the attractor in the directions previously characterized by zero thickness. The smallest of such average thicknesses is nothing but the critical distance ε^* one must reach to observe $D_{\text{cg}} = L$ (in this simplified approach the dependence of the exponential rate on the accuracy f is missing). By assuming a small amplitude of the external noise ξ , we can linearize around the equilibrium position, thus obtaining a typical Langevin equation (we assume the time to be a continuous variable, for simplicity)

$$\dot{u} = \lambda u + \xi, \quad (5.7)$$

where λ is the associated (negative) Lyapunov exponent. By also assuming ξ to be delta-correlated with a diffusion coefficient \mathcal{D} , we find that the width of the distribution of u -values is given by $\delta u = \sqrt{-\mathcal{D}/\lambda}$. The problem is now to find the hidden dependence of δu on L . As the Lyapunov exponents are asymptotically independent of the chain length, we have to consider the diffusion coefficient \mathcal{D} . The simplest hypothesis one can make is that of equal contributions of the external noise to the evolution of each degree of freedom. This leads to assuming \mathcal{D} to be inversely proportional to the space dimension L . Accordingly, the thickness of the attractor δu should decay as $L^{-1/2}$, a behaviour much slower

than the observed exponential one. This indicates that the hypothesis of the equipartition of the thermal noise contribution fails. This point will be the subject of future research.

More recently, Mayer-Kress and Kaneko [6] reconsidered the problem of estimating the effect of coupling with nearby points onto the dynamical evolution at a given site, to justify the slow increase of the fractal dimension observed for increasing the embedding dimension L . However, we do not see how it is possible to relate a typical dynamical indicator like the growth rate of infinitesimal disturbances (evaluated through the spectrum of Lyapunov exponents measured in a moving reference frame [23]), with a property of the (static) invariant measure, like the fractal dimension. In the case of the Kaplan–Yorke formula it was possible to find such a link because of the closure of the equations in phase space. Here, instead, as we are looking at a subset of the space, we always neglect the coupling with the remaining degrees of freedom whose effect is precisely what we are trying to determine. If one is interested in showing the equivalence between the dynamical behaviour of an (in principle) infinite chain and many finite (sufficiently long) pieces, the main question to be answered is the estimation of the effect of a functional perturbation of a given set of equations (namely the coupling with additional maps), which is not the same as studying the effect of a perturbation on the initial condition, which is the effect measured by the Lyapunov exponents.

6. Short-length chains

In a discussion of the fractal structure of a chain of maps it is worth investigating the validity of the Kaplan–Yorke relation. There is no reason to expect an agreement between Lyapunov dimension and information dimension in presence of a noninvertible dynamics as in the case of the logistic maps considered in this paper. In fact, invertibility is very crucial in that it guarantees

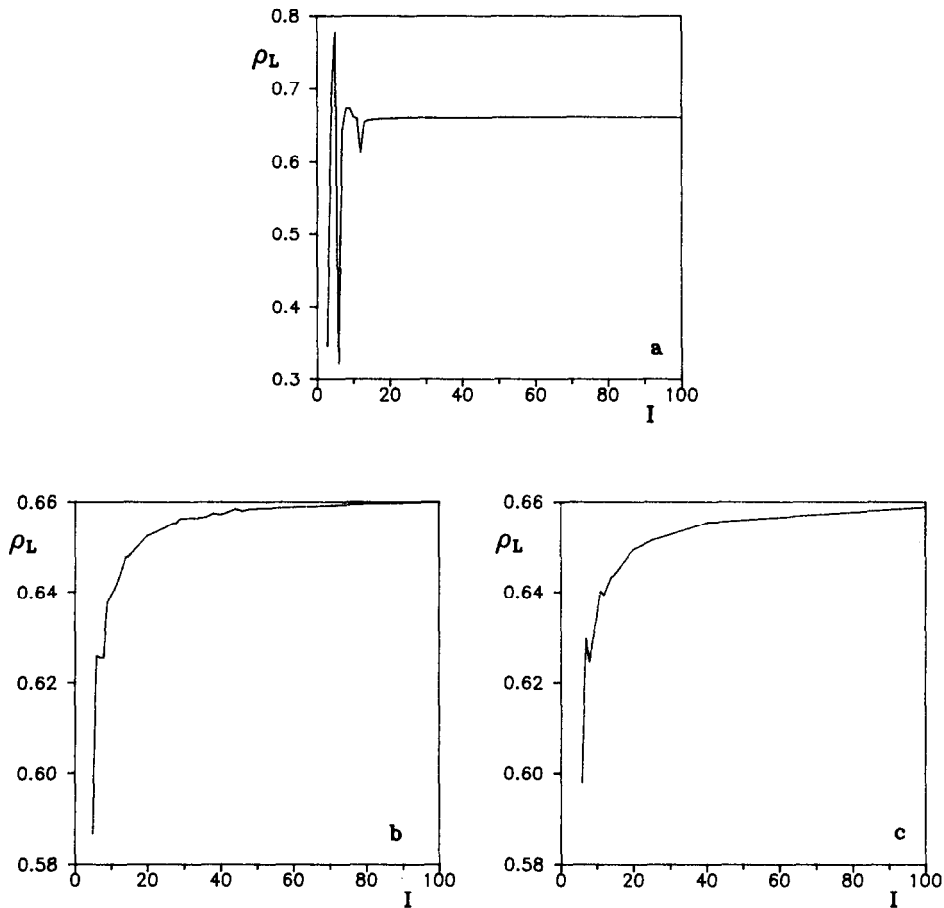


Fig. 10. Dimension density ρ_L , estimated from the Lyapunov spectrum, for chains of tent maps of increasing length I , with (a) periodic, (b) antiperiodic and (c) fixed boundary conditions.

that an initial partition of the attractor with nonoverlapping elements is still such after iterating all the elements. Previous simulations performed for the Sinai map [24] indicated that the Lyapunov dimension is strictly larger than the information dimension as estimated with the nearest-neighbour algorithm. Our numerical analysis has been performed by using tent maps ($x_{n+1}^i = 1 - 2|y_n^i - \frac{1}{2}|$) to avoid difficulties related to the presence of singularities in the invariant measure. It indicates that if there is any difference it is small and remains finite for increasing L .

As direct computations of the fractal dimension can be performed only for low-dimensional attractors, we have first investigated the convergence of the Lyapunov spectrum (for two different values of the coupling constant ε) for increasing length of the chain, from $L = 2$ to $L = 100$. Large fluctuations of the dimension density ρ_L have been observed up to $L = 20$ (to be compared with $L = 50$ for logistic maps) due to the presence of several periodic windows. To decrease such fluctuations we have changed boundary conditions choosing antiperiodic ($x^0 = -x^L$; $x^{L+1} = -x^1$) and fixed ($x^0 = x^L = \bar{x}$) con-

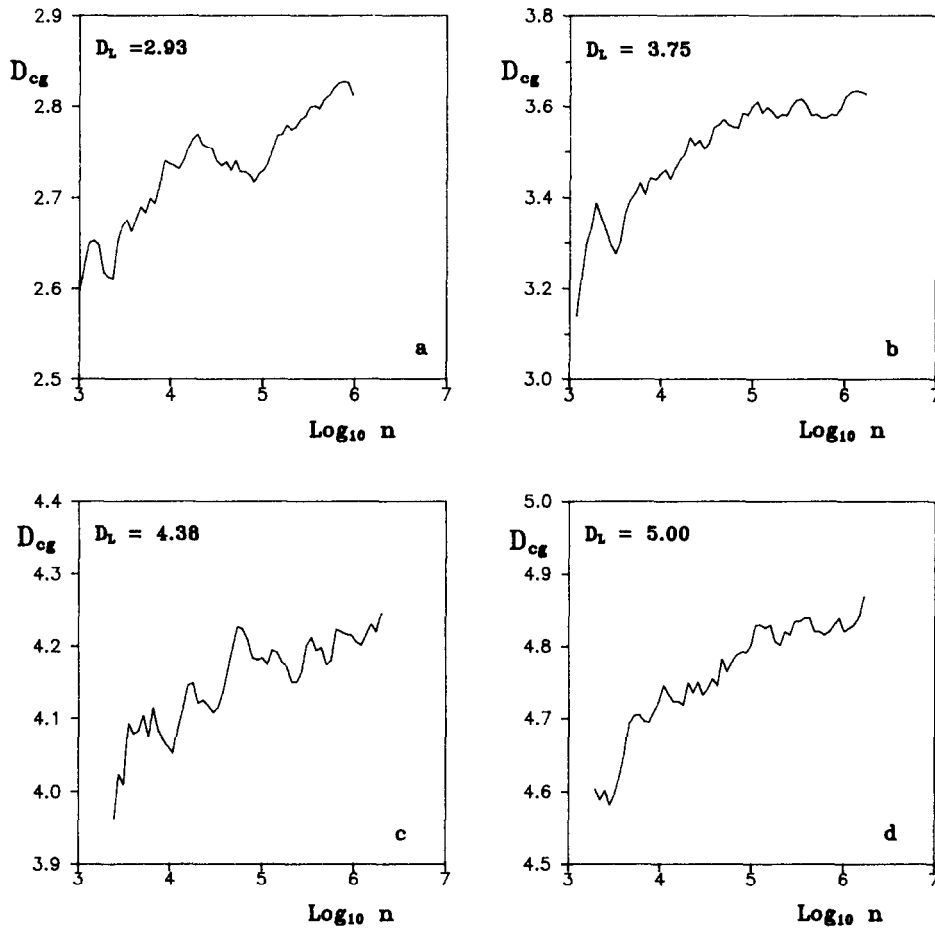


Fig. 11. Coarse grained dimension for chains of coupled tent maps with antiperiodic boundary conditions: (a), (b) and (c) refer to $\varepsilon = \frac{2}{3}$ and $I = 5, 6,$ and $7,$ respectively; (d) to $\varepsilon = \frac{1}{3}$ and $I = 5.$ All curves are estimated from the distance of the 4th neighbour.

ditions. The results reported in fig. 10 for $\varepsilon = \frac{2}{3}$ both indicate that the oscillations due to periodic structures almost disappear and show a convergence to the same dimension density $\rho_L = 0.660$ regardless of the boundary conditions.

Then, we have estimated the information dimension D with the nearest neighbour method for antiperiodic boundary conditions. We have again encountered a very slow convergence, forcing us to consider short chains only. First, we have considered three cases where D_L is less than the length of the chain ($\varepsilon = \frac{2}{3}$ and $I = 5, 6, 7$). Then we have analyzed a situation where the sum of all Lyapunov exponents is still positive ($\varepsilon = \frac{1}{3}$

and $I = 5$), so that the upper limit to D is given by the dimension I of the space considered. The numerical results are presented in fig. 11, all referring to the 4th neighbour. All of the four curves are slightly below the upper bound given by the Lyapunov dimension (in the worst case the difference is 0.14), but none has reached saturation, so that we can argue that if there is any difference it is very small. More important, it seems that such a difference does not increase for increasing I . Thus, we can conclude that, despite the global noninvertibility of model (2.1), (2.2), the asymptotic attractor where the invariant measure is sitting on, is presumably characterized by

an almost completely invertible dynamics, reinforcing the hypothesis that a chain of logistic maps can be effectively used as a simplified model to understand spatio-temporal phenomena.

7. Conclusions

In this paper we have presented a detailed numerical analysis of the fractal properties of the invariant measure in the case of a 1D chain of diffusively coupled maps. We can conclude stating that it is not possible to distinguish a stochastic signal from a spatio-temporal chaotic behaviour relying on the estimate of dimension in suitable embedding spaces. Nevertheless, the slow convergence of the coarse-grained dimension indicates nontrivial properties of the invariant measure, whose complete understanding requires a strictly local analysis of the phase space. We should also mention that use of the Grassberger–Procaccia algorithm leads to analogous results for spatial embedding, whereas it leads to incomprehensible oscillations in the temporal case. Such a further difficulty points in the direction that multifractal corrections might play a relevant role in determining the asymptotic measure, and, in turn, a statistical mechanics description in the infinite length limit.

Acknowledgements

We acknowledge useful discussions on the application of orthogonal decomposition with F. Giovannini. We also wish to thank P. Grassberger for having provided us an efficient code to estimate fractal dimensions which we used to construct an analogous program for the nearest-neighbour algorithm.

References

- [1] J.-P. Eckmann and D. Ruelle, *Rev. Mod. Phys.* 57 (1985) 617.
- [2] P. Grassberger, R. Badii, and A. Politi, *J. Stat. Phys.* 51 (1988) 135.
- [3] P. Paoli, A. Politi, and R. Badii, *Physica D* 36 (1989) 263.
- [4] Y. Pomeau, A. Pumir, and P. Pelce, *J. Stat. Phys.* 37 (1984) 39;
K. Kaneko, *Prog. Theor. Phys.* 74 (1985) 1033;
R. Livi, A. Politi, and S. Ruffo, *J. Phys. A* 19 (1986) 2033;
J.-P. Eckmann and C.E. Wayne, *J. Stat. Phys.* 50 (1988) 853.
- [5] P. Grassberger, *Physica Scripta* 40 (1989) 346.
- [6] G. Mayer-Kress and K. Kaneko, *J. Stat. Phys.* 54 (1989) 1489.
- [7] A. Politi, G. D'Alessandro, and A. Torcini, in: *Measures of Complexity and Chaos*, eds. N.B. Abraham et al. (Plenum, New York, 1989) p. 409.
- [8] K. Kaneko, *Prog. Theor. Phys.* 72 (1984) 480.
- [9] R. Badii and A. Politi, *Phys. Rev. Lett.* 52 (1984) 1661.
- [10] E. Ott, W. Withers, and J.A. Yorke, *J. Stat. Phys.* 36 (1984) 687.
- [11] J. Guckenheimer, *Contemp. Math.* 28 (1984) 357;
I. Dvorak and J. Klaschka, *Phys. Lett.* 145 A (1990) 225;
J.B. Ramsey and H.-J. Yuan, *Phys. Lett.* 134 A (1989) 287.
- [12] G. Mayer-Kress, in: *Directions in Chaos*, ed. Hao Bai-Lin (World Scientific, Singapore, 1987).
- [13] J. Theiler, *Phys. Rev. A* 36 (1987) 4456.
- [14] P. Grassberger and I. Procaccia, *Phys. Rev. Lett.* 50 (1983) 346.
- [15] J.-P. Eckmann and D. Ruelle, *Fundamental limitations for estimating dimensions and Lyapunov exponents in dynamical systems*, preprint.
- [16] N. Aubry, P. Holmes, J.L. Lumley and E. Stone, *J. Fluid. Mech.* 192 (1988) 115; *Physica D* 38 (1989) 1.
- [17] L. Sirovich, *Physica D* 37 (1989) 126.
- [18] S. Ciliberto and Nicolaenko, *Europhy. Lett.*, to appear.
- [19] D.S. Broomhead and G.P. King, *Physica D* 20 (1986) 217.
- [20] A.I. Mees, P.E. Rapp, and L.S. Jennings, *Phys. Rev. A* 36 (1987) 340.
- [21] G. Mayer-Kress and T. Kurz, *Complex Systems* 1 (1987) 821.
- [22] Y. Pomeau, *Compt. Rend. Acad. Sci. Paris*, t. 300, Série II, 7 (1985) 239.
- [23] R.J. Deissler and K. Kaneko, *Phys. Lett.* 119 A (1987) 397.
- [24] R. Badii and A. Politi, in: *Fractals in Physics*, eds. L. Pietronero and E. Tosatti (Elsevier, Amsterdam, 1986) p. 453.